Transmission Surface Plasmon Resonance (T-SPR) Spectroscopy

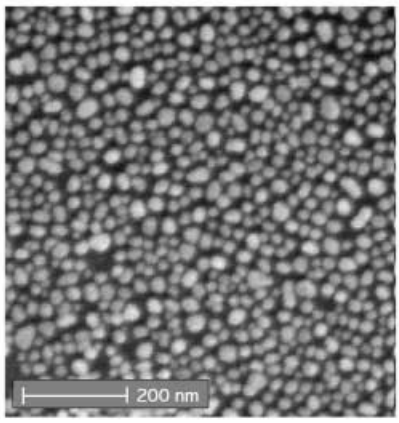

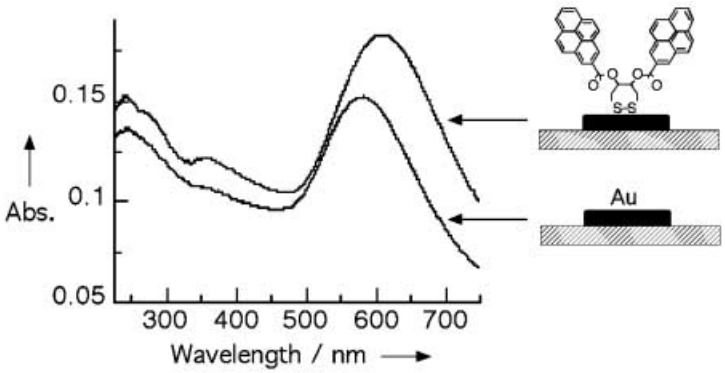

Au island films evaporated on transparent substrates are used to sense molecular binding to the Au surface. For more details see following pages.

Monitoring Self-Assembly Processes: Toward Sensing Applications

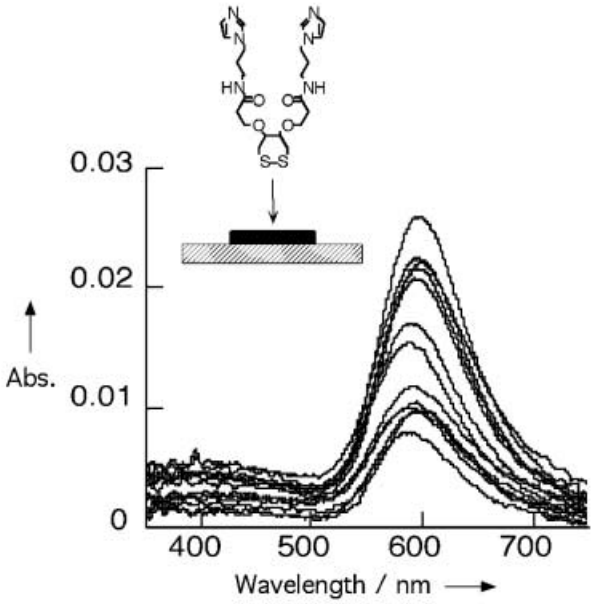

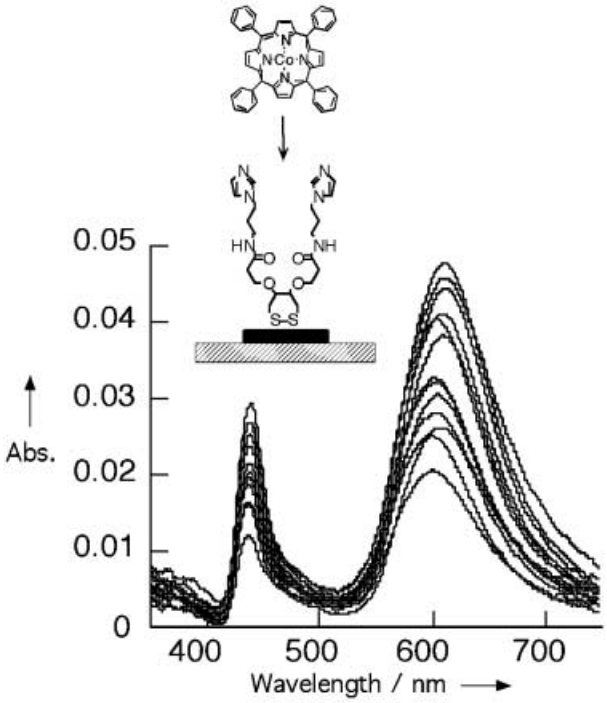

  0947-6539/02/0817-3849 $ 20.00+.50/0

Transmission Surface-Plasmon Resonance (T-SPR) Measurements for Monitoring Adsorption on Ultrathin Gold Island Films

Gregory Kalyuzhny, Alexander Vaskevich, Marie Anne Schneeweiss, and Israel Rubinstein*[a]

Abstract: Evaporation of ultrathin (1.3 – 10 nm nominal thickness) gold films onto quartz or mica leads to the formation of a layer of rather uniform gold islands on the transparent support. The morphology of ultrathin gold island films of various thicknesses was studied by using atomic force microscopy (AFM) and scanning electron microscopy (SEM) imaging. The surface plasmon (SP) absorption characteristic of such films is highly sensitive to the surrounding medium, with the plasmon band changing in intensity and wavelength upon binding of various molecules to the surface. The binding process can be monitored quantitatively by measuring the changes in the gold SP absorption, by using transmission UV/Vis spectroscopy. The method, termed transmission surface plasmon resonance (T-SPR) spectroscopy, is shown to be applicable to both chemically and physically adsorbed molecules, in liquid or gas phase, with measurements carried out either ex situ or in situ (real-time measurements) using a variety of molecular probes. Binding to a preformed molecular layer on the Au surface produces a similar response, suggesting the possible use of T-SPR for selective sensing. The sensitivity of T-SPR spectroscopy in detecting molecular binding to the gold depends strongly on the film preparation conditions, and may be comparable to that obtained in surface plasmon resonance (SPR) sensing.

Keywords: adsorption · gold · self-assembly · sensors · surface plasmon resonance spectroscopy · UV/Vis spectroscopy

Introduction

Thin Au films evaporated onto transparent substrates exhibit structure-dependent UV/Vis transmission spectra.[1, 2] Continuous films with a small roughness show a minimum absorbance around 550 nm. Such films are used as optically transparent electrodes in spectroelectrochemistry,[3, 4] as well as substrates for molecular self-assembly, and allow characterization of monolayers containing chromophores by transmission UV/Vis spectroscopy.[5–15] On the other hand, ultrathin (ca. = 10 nm) *island-type* Au films deposited on transparent substrates exhibit transmission spectra that are strikingly different, showing an absorption band attributed to excitation of the surface plasmon (SP), similar to various systems consisting of dispersed Au particles.[1, 2] The morphology of such films is controlled by the evaporation parameters.[15–18]

The notable sensitivity of the SP excitation to the presence of adsorbates, which is derived from the general dependence of the SP band position and amplitude on the refractive index of the contacting medium, triggered the construction of various chemical and biological sensors based on SP measurements. Traditionally, surface plasmon resonance (SPR) measurements are carried out in the reflection mode using the Kretschmann configuration,[19] although other arrangements, including optical waveguides or diffraction gratings, were also reported.[20–22] SPR sensing usually requires rather complicated and expensive optical equipment. SP absorbance can be also detected by measuring UV/Vis transmission spectra. Optical sensors based on the latter approach can be constructed as a layer of Au nanoparticles deposited on a transparent support.[23–25] An approach based on relatively thick (ca. 100 nm) island films evaporated through a mask of polystyrene spheres was developed by Van Duyne and coworkers.[26, 27]

The use of ultrathin ($\leq$10 nm) evaporated Au island films, demonstrated here, presents an effective means for monitoring changes in the immediate environment of the Au, and more specifically, formation of (sub)monolayers of adsorbed species. Unlike Au colloids and colloid films, the evaporated Au island films do not require the use of stabilizing molecules

[a] Prof. I. Rubinstein, G. Kalyuzhny,[+] Dr. A. Vaskevich, Dr. M. A. Schneeweiss[++]
Department of Materials and Interfaces
Weizmann Institute of Science
Rehovot 76100 (Israel)
Fax: (+972) 8-9344137
E-mail: israel.rubinstein@weizmann.ac.il

[+] Present address: Department of Chemistry, University of Texas at Austin, Austin, TX 78712 (USA)

[++] Present address: L.O.T-Oriel Ltd., 1 Mole Business Park, Leatherhead, Surrey, KT22 7BA (UK)

  0947-6539/02/0817-3850 $ 20.00+.50/0

and avoid the stage of nanoparticle immobilization on a support,[16–18, 28, 29] thereby simplifying the preparation procedure. As recently shown by us,[18] changes in the SP band accompanying molecular binding to the Au surface are obtained directly from transmission UV/Vis spectra, and correlate with the surface coverage. The method, termed transmission surface plasmon resonance (T-SPR) spectroscopy, is shown to be general and effective in monitoring chemical or physical adsorption onto the Au films both in situ and ex situ, with a sensitivity (based on the use of conventional UV/Vis spectrophotometers) approaching values characteristic of SPR sensing.

Results and Discussion

Ultrathin gold island films on transparent substrates

Atomic force microscopy: Figure 1 and Figure 2 show AFM images (non-contact mode) of ultrathin gold films on quartz and mica, with nominal thicknesses of 1.3, 2.5, 5.0, and 10.0 nm, evaporated at 0.005 – 0.01 nm s^{-1}. The left, center, and right columns in Figure 1 and 2 show typical images of samples which were unannealed, annealed for 4 h at 250 °C, and annealed for 12 h at 350 °C, respectively. The overall morphology of the films evaporated on quartz and mica is qualitatively similar. The average island size increases with the nominal thickness, as previously found for ultrathin gold

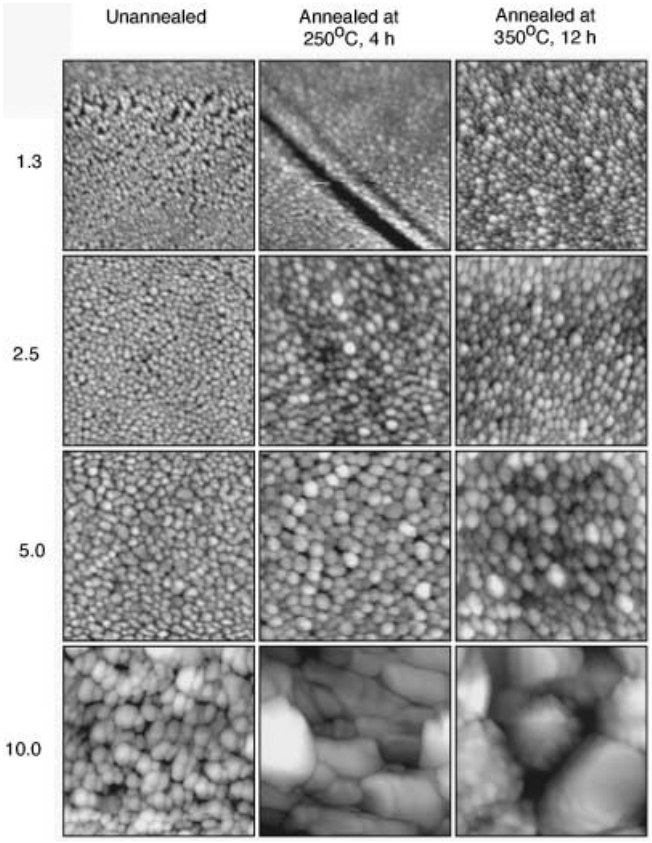

Figure 1. Tapping mode AFM topographic images of ultrathin gold films on quartz (500 nm scan). Nominal thicknesses (left, in nm) and preparation conditions (top) are indicated.

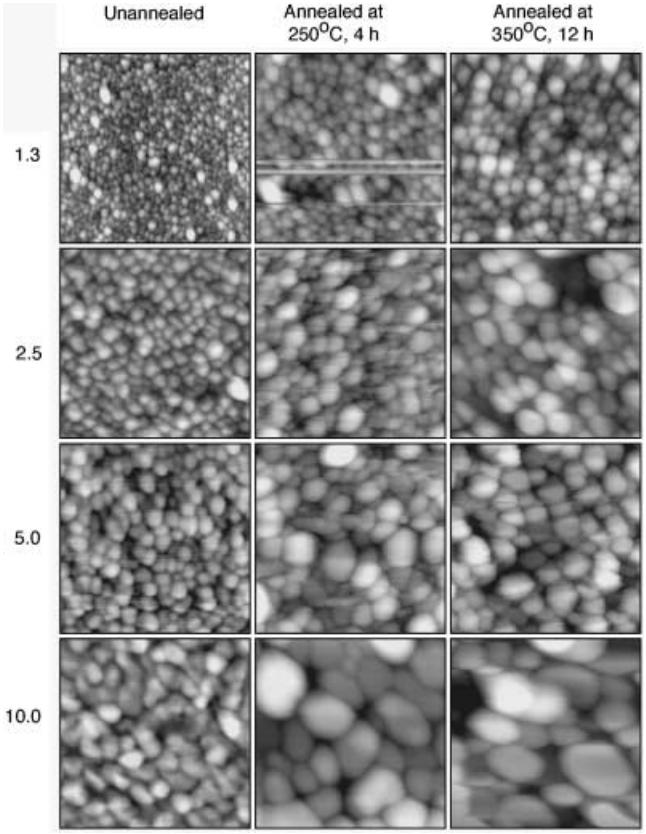

Figure 2. Tapping mode AFM topographic images of ultrathin gold films on mica (500 nm scan). Nominal thicknesses (left, in nm) and preparation conditions (top) are indicated.

films evaporated on mica at faster rates (0.02 – 0.04 nm s^{-1}).[16] Annealing generally leads to an increase in the average diameter of the islands and to an increase of the surface roughness (the latter not shown here). Films obtained by using the two annealing procedures differ considerably only for the highest nominal thickness (10.0 nm) on quartz, where large aggregates of smaller islands are observed. The more extensively annealed (12 h, 350 °C) films show lower stability with respect to rinsing with various solvents; the latter is more pronounced with films evaporated on quartz.

Note that the values of nominal thickness given here may not be accurate due to the different sticking coefficient of gold atoms to different substrates. An unequivocal comparison of morphology and UV/Vis spectra (see below) of the films evaporated on quartz and mica is, therefore, not possible. With thicker films this effect becomes insignificant.

A typical particle size for each sample was determined by measuring the diameter of approximately 20 randomly selected islands and calculating their average diameter. (Quantitative analysis of the Au island size and distribution could not be obtained by the image analysis software due to difficulties in defining the grain boundaries.) The results given in Table 1 confirm the general trends noted above. Except for the thickest films, the standard deviation of the island size is consistently smaller for films evaporated on quartz than for the corresponding films evaporated on mica. It is important to note that the island size values given in Table 1 are likely to be overestimated, as a result of tip convolution.

  0947-6539/02/0817-3851 $ 20.00+.50/0

Table 1. Average Au island size and distribution obtained from AFM images. All the measurements were performed manually (see text).

Substrate	Annealing conditions	Nominal thickness [nm]	Average island diameter [nm]	Standard deviation of island size [nm]	Islands per unit surface area [nm^{-2}]
quartz	unannealed	1.3	8.4	1.4 (17%)	4.2×10^{-3}
		2.5	15.2	2.7(18%)	3.2×10^{-3}
		5.0	25.6	5.7(22%)	1.6×10^{-3}
		10.0	38.6	9.8(25%)	5.3×10^{-4}
	4 h at 250 °C	1.3	14.2	2.7(19%)	4.3×10^{-3}
		2.5	22.0	3.9(18%)	1.6×10^{-3}
		5.0	32.9	5.7(17%)	1.1×10^{-3}
		10.0	99.9	37.9(38%)	1.0×10^{-4}
	12 h at 350 °C	1.3	11.2	3.8(34%)	2.4×10^{-3}
		2.5	18.6	6.5(35%)	1.7×10^{-3}
		5.0	28.8	9.2(32%)	6.2×10^{-4}
		10.0	173.9	53.3(31%)[a]	3.6×10^{-5}[a]
mica	unannealed	1.3	12.0	3.9(33%)	2.5×10^{-3}
		2.5	29.8	9.2(31%)	9.0×10^{-4}
		5.0	28.3	9.2(33%)	6.2×10^{-4}
		10.0	43.3	11.6(27%)	2.9×10^{-4}
	4 h at 250 °C	1.3	23.2	5.8(25%)	9.0×10^{-4}
		2.5	42.4	12.0(28%)	3.7×10^{-4}
		5.0	49.7	21.3(43%)	3.5×10^{-4}
		10.0	87.0	30.2(35%)	1.1×10^{-4}
	12 h at 350 °C	1.3	36.4	10.2(28%)	5.6×10^{-4}
		2.5	54.2	12.8(24%)	2.9×10^{-4}
		5.0	57.6	13.5(23%)	2.6×10^{-4}
		10.0	93.5	33.3(36%)	8.0×10^{-5}

[a] Agglomerates of small islands are treated as single islands.

This is evident in Figure 3, where an environmental scanning electron microscopy (E-SEM) image of one of the films (5.0 nm Au on mica, annealed) is shown. While the island distribution imaged by E-SEM (Figure 3) and AFM (Figure 2) is similar, the Au islands in Figure 3 appear smaller in diameter and more separated. This difference is due to tip convolution (AFM) and contrast limitations (E-SEM); hence, the true island shape probably lies somewhere between the two.

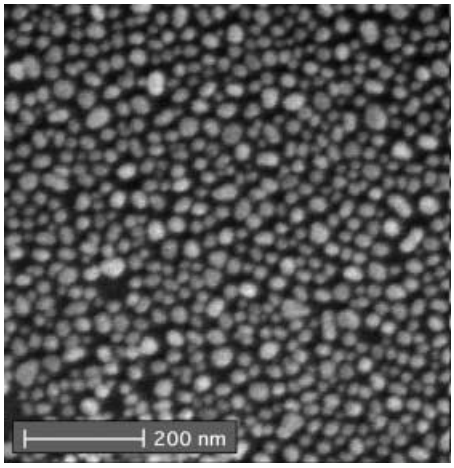

Figure 3. E-SEM image of an ultrathin gold film on mica (5.0 nm nominal thickness, annealed 4 h at 250 °C).

UV/Vis spectroscopy: T-SPR spectra of unannealed and annealed[30] Au films on quartz and mica are shown in Figure 4. In all cases the films exhibit a defined gold surface plasmon (SP) band, which shifts to the red as the nominal thickness increases. The band intensity is approximately linearly correlated with the film nominal thickness (Figure 4, insets) for both annealed and unannealed films in the thickness range 1.3 – 5.0 nm, while the intensity is always greater for the unannealed films.

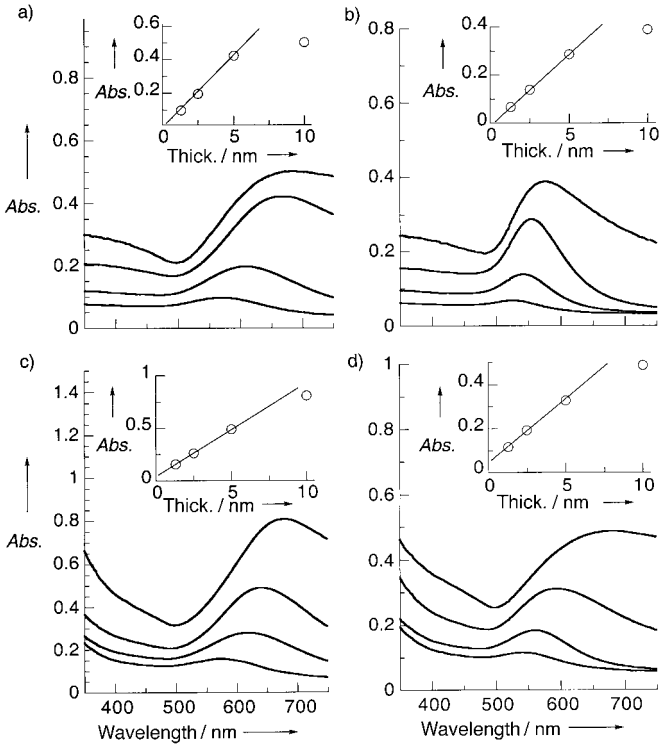

Figure 4. UV/Vis spectra of ultrathin gold films on quartz (a, b) and on mica (c, d), unannealed (a, c) or annealed 4 h at 250 °C (b, d). Nominal thickness: 1.3 nm (bottom curves), 2.5 nm, 5.0 nm, 10 nm (top curves). Insets: Dependence of the band intensity on the Au nominal thickness.

Adsorption on gold island films

The studied molecules: The choice of adsorbing molecules was partly based on the observation that certain thiols (e.g., 4-aminothiophenol, 4-mercaptopyridine) caused gradual change in the Au spectrum after adsorption on ultrathin Au films, which may be attributed to slow modification of the island morphology, or some removal of Au, as a result of thiol adsorption. This effect is not seen (or is marginal) with the cyclic disulfides and long-chain thiols **1** – **5** used in this work.

T-SPR measurements: The method is based on the measurement of transmission UV/Vis spectra of the same Au island film before and after adsorption. It is effectively demonstrated by monitoring the formation of a monolayer of **1** on a 2.5 nm Au island film on quartz. Adsorption of **1** results in both an increase in the SP band intensity and a red shift of the absorbance maximum (Figure 5a). The effect of the adsorption is seen more clearly in the difference spectrum (Figure 5b), obtained by subtraction of the spectra in Figure 5a.

0947-6539/02/0817-3852 $ 20.00+.50/0 *Chem. Eur. J.* **2002**, *8*, No. 17

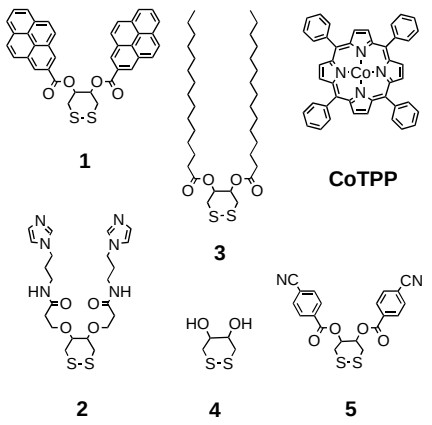

The maximum intensity of the difference spectrum is referred to as the plasmon intensity change (PIC). The difference spectrum (Figure 5b) shows the evolution of both the molecular absorption of the pyrene chromophore in the UV region, and the gold SP band in the visible region.[16, 18] Binding of **1** to the gold can be monitored by following the position or the intensity of the SP maximum, and quite conveniently by monitoring the PIC. As shown previously,[18] all three parameters (intensity and wavelength of the SP band; the PIC) are proportional to the change in molecular absorbance (hence, to the surface coverage).

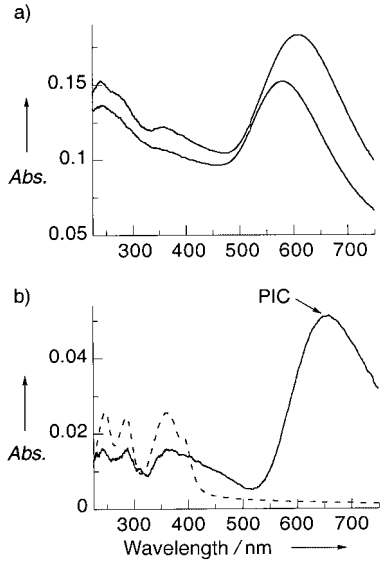

Figure 5. a) Transmission UV/Vis spectra of an unannealed Au substrate (2.5 nm nominal thickness, evaporated on quartz) before (bottom curve) and after (top curve) immersion in 2 mM solution of **1** in $CHCl_3$ for 49 min. b) Difference spectrum, obtained by subtraction of the bottom spectrum from the top one in a; the dashed line is a spectrum of a thick layer of **1**, obtained by evaporation of a drop on quartz (original spectrum divided by 6).

Self-assembled monolayers of 2: Another illustration of the correlation between the PIC and the molecular absorbance of monolayers is given by the formation of self-assembled monolayers (SAMs) of **2** incorporating chromophores such as CoTPP. The ligand **2** possesses two imidazolyl residues that can effectively bind metallomacrocycle molecules by axial coordination.[16, 31, 32] CoTPP can be bound to a SAM of **2** by forming a stable complex with one imidazole group.[16] We have previously demonstrated[16] that binding of CoTPP to a SAM of **2** on Au island films can be monitored by transmission UV/Vis spectroscopy. The process was monitored quantitatively by measuring simultaneously the evolution of the Soret band of the porphyrin and the PIC accompanying the binding process. As in the case of the adsorption of **1** discussed above, a correlation between the amount of bound CoTPP and the PIC was shown.[16]

Here the use of T-SPR for studying adsorption on Au of molecules that do not possess a chromophore is exemplified by monitoring the kinetics of formation of a monolayer of **2** on an Au island film, using CoTPP binding as a 'development' tool. Direct monitoring of the adsorption of **2** using the SP absorbance can be confirmed by subsequent binding of CoTPP and measurement of the amount of bound CoTPP.

Formation of a SAM of **2** is accompanied by a respective change in the Au SP band, as shown in Figure 6a. Subsequent binding of CoTPP to the fractional monolayers of **2** is manifested by the appearance of the Soret band of the porphyrin, as well as an additional change in the SP absorbance (Figure 6b), resulting from further alteration of the refractive index of the contacting medium. As seen in Figure 6c, the increase in the Au PIC associated with the kinetics of adsorption of **2** is fully consistent with both the Soret band absorption of the bound CoTPP and the additional enhancement of the Au plasmon resulting from CoTPP binding. This result demonstrates the use of transmission surface plasmon measurements for monitoring indirect binding of an analyte to a receptor layer on the Au surface, suggesting use of the method for selective sensing.

Self-assembled monolayers of 3: Self-assembly of **3** on Au island films is another example of the use of T-SPR measurements for monitoring adsorption of transparent molecules, as well as for establishing a relationship between the PIC and the surface coverage. In addition to measuring the change in the Au SP band accompanying self-assembly of **3**, the hydrophobic nature of the alkyl chains enables qualitative monitoring of the adsorption process by measuring the change in the water contact angle (CA). As seen in Figure 7a, the change in the advancing water CA and the PIC with adsorption time show very similar kinetics, although the relationship between surface coverage and contact angle is not necessarily linear as found here (Figure 7b). This result provides an additional indication of the general correlation between the Au PIC and surface coverage by the adsorbed molecule.

In situ measurements in liquid and gas phase: T-SPR measurements can be applied to in situ quantitative monitoring of adsorption on Au island films. Figure 8 shows the kinetics of chemisorption of a SAM of 1-decanethiol ($C_{10}SH$) on a 5 nm unannealed Au island film evaporated on mica, from solution and from the gas phase. The measurement was carried out by recording the absorbance at a single wavelength (720 nm), chosen to be close to the PIC maximum (the latter was determined separately by measuring the spectra of

  0947-6539/02/0817-3853 $ 20.00+.50/0

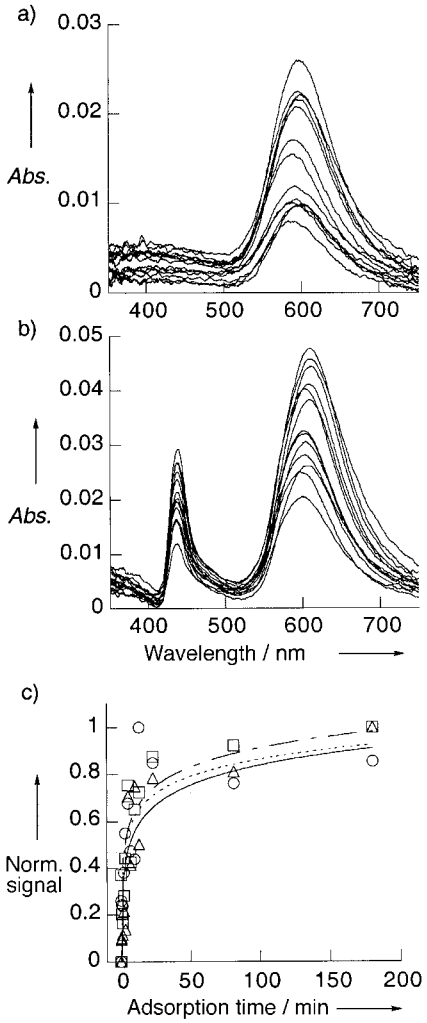

Figure 6. a) UV/Vis spectra of SAMs of **2** adsorbed from 0.4 mM solution in $CHCl_3$ for 1 s – 180 min (each curve is a different sample); b) UV/Vis spectra of the SAMs in a after binding of CoTPP from 1.0 mM solution of the porphyrin in $CHCl_3$ for 10 min; c) normalized quantities of the various absorption bands versus adsorption time: △: PIC after adsorption of **2** (data from a); PIC (□) and Soret band (○) absorbance accompanying CoTPP binding to the SAMs of **2** (data from b). The lines shown in c are logarithmic fittings of the experimental data. The Au substrates were 2.5 nm (nominal thickness), evaporated on mica and annealed 4 h at 250 °C.

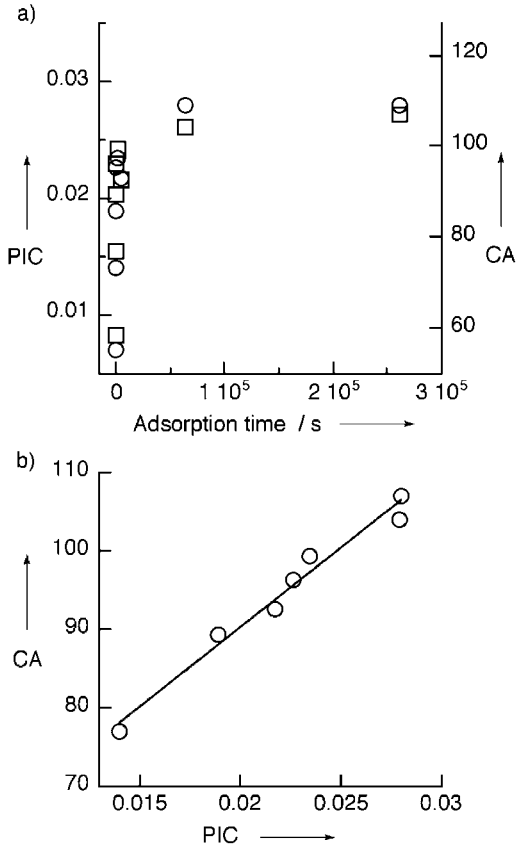

Figure 7. a) Kinetics of formation of a SAM of **3** adsorbed from 2 mM solution in $CHCl_3$. The Au PIC (□) and the water CAs (○) are plotted versus adsorption time; b) correlation between the PIC and water CAs (data from a). All the experimental points were measured on the same sample. The line shown in b is a linear fitting of the experimental data. The Au substrate was 2.5 nm (nominal thickness) on quartz, unannealed.

a similar Au island film before and after adsorption of a full monolayer). Introduction of $C_{10}SH$ results in an increase in the absorption at 720 nm, eventually reaching a steady state (Figure 8a, 8b). The PIC (at 720 nm) accompanying $C_{10}SH$ adsorption from the gas phase is substantially greater than the one obtained in solution (compare Figure 8a and b). This is attributed to the greater difference in dielectric constants of $C_{10}SH$ ($\varepsilon = 2.126$) and air ($\varepsilon = 1$) versus 2,2,2-trifluoroethanol (TFE; $\varepsilon = 1.664$), or to possible deposition of more than one monolayer of $C_{10}SH$ in the gas phase, or to a combination.

The same kind of in situ measurements enable us to monitor physical adsorption on Au island films. This is exemplified by monitoring the Au PIC during adsorption of benzene and pyridine in the gas phase onto 5 nm unannealed Au films evaporated on mica (Figure 9). The steady state is reached faster for benzene than for pyridine, probably due to the higher vapor pressure of benzene than of pyridine (boiling

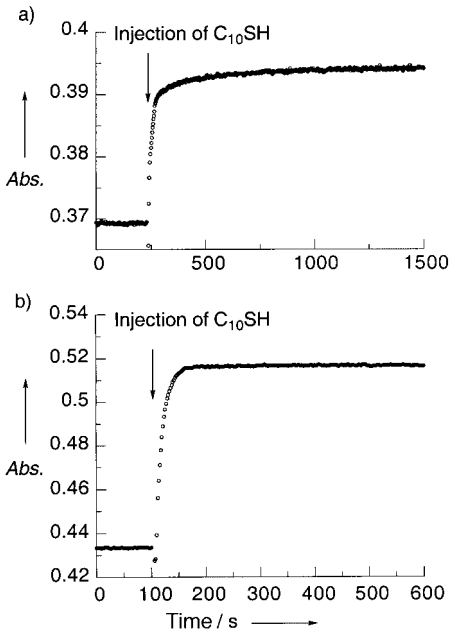

Figure 8. Kinetics of formation of a SAM of $C_{10}SH$ on a 5 nm unannealed Au film evaporated on mica, adsorbed from 2 mM solution in CF_3CH_2OH (a) and from gas phase (b). The absorbance at 720 nm is shown as a function of adsorption time. The arrows indicate the time of injection of $C_{10}SH$.

0947-6539/02/0817-3854 $ 20.00+.50/0 *Chem. Eur. J.* **2002**, *8*, No. 17

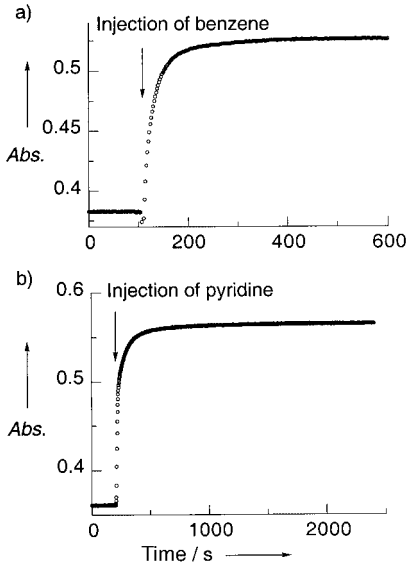

Figure 9. Kinetics of adsorption from gas phase of benzene (a) and pyridine (b) on a 5 nm unannealed Au film evaporated on mica. The absorbance at 720 nm is shown as a function of adsorption time. The arrows indicate the time of injection of the adsorbing molecules.

temperatures: 80.1 °C and 115.6 °C, respectively). As in the case of $C_{10}SH$ adsorption, the amount of physisorbed molecules may exceed one monolayer.

The same kind of in situ T-SPR measurements, either in solution or in the gas phase, were also carried out with 1-hexadecanethiol ($C_{16}SH$), 4-aminothiophenol and various additional cyclic disulfides, with qualitatively similar results.

It is important to consider here whether the change in the SP absorption at a single wavelength is truly proportional to the amount of adsorbed molecules. While this may be a good approximation in many cases, the situation is more problematic with systems in which adsorption is accompanied by a considerable shift of the SP maximum. In such cases, more quantitative in situ results may be obtained by recording a series of spectra and determining the PIC or related parameters.[18]

Choosing the appropriate Au substrate for T-SPR spectroscopy: As shown above, the morphology and optical properties of ultrathin Au island films depend strongly on the preparation conditions, that is, nominal thickness and annealing. To find the optimal conditions for monitoring molecular self-assembly with maximum sensitivity and reproducibility, a set of ultrathin Au films of nominal thicknesses of 1.3, 2.5, 5, and 10 nm were studied as substrates for SAMs of **3**, prepared by using identical adsorption parameters (Table 2). Some of the slides were annealed for 4 h at 250 °C.

As seen in Table 2, the PIC (hence, the sensitivity) is considerably greater with unannealed Au films than with annealed films. For unannealed Au films the sensitivity improves with nominal thickness, reaching a plateau at 5–10 nm, while for annealed films the best sensitivity is at 5 nm. The smaller PIC values observed with annealed films led to lower reproducibility than with unannealed films, and became unreliable at 10 nm. The highest sensitivity, obtained with unannealed Au films of 10 nm thickness, is 0.7 % of a monolayer, comparable to the sensitivity of SPR spectroscopy.[22]

Table 2. The PIC obtained with various Au island films for the formation of a SAM of **3**, adsorbed from 2 mM solution in $CHCl_3$ for 40 min.

Nominal thickness [nm]	Annealing conditions	PIC maximum (average of 4 samples)	Standard deviation [%]	Sensitivity (% of a monolayer)
1.3	unannealed	0.021	7	5
	4 h at 250 °C	0.005	4	20
2.5	unannealed	0.057	7	2
	4 h at 250 °C	0.010	18	10
5.0	unannealed	0.121	9	0.8
	4 h at 250 °C	0.012	13	8
10	unannealed	0.148	4	0.7
	4 h at 250 °C	0.005	78	20

While unannealed Au island films are the substrates of choice for SP measurements, the weaker PIC response of the annealed films makes them better substrates for conventional transmission UV/Vis spectroscopy of SAMs, as the lower Au absorption implies better resolution of the monolayer absorption. Annealed Au films are also generally more stable in various solvents. It is therefore concluded that the choice of Au substrate should be determined by the nature and requirements of the specific experiment; the data given in Table 2 provide a good guideline.

Comparing the PIC obtained with various SAMs: The PIC obtained for SAMs comprising different molecules should be generally different. Factors other than surface coverage that may affect the SP absorption include, for example, refractive index, dipole moment, type of binding to the Au surface, and molecular structure (size, electron π systems, chromophores, etc.). Understanding the different effects is beyond the scope of the present work; however, analysis of the PIC associated with formation of SAMs of the series of cyclic disulfides **1-5** provides some indications. The common cyclic disulfide attachment group allows one to assume similar binding to the Au surface. The molecules were adsorbed on similar Au island films from 2 mM solutions for the same amount of time (40 min, sufficient to achieve $\geq$95 % of a monolayer coverage). This comparison is only semiquantitative, as the molecular arrangement and density vary for different molecules.

Figure 10 shows the Au PIC for the molecules **1**–**5**. While the correlation with molecular weight is evident, other factors seem to be less important in this case. For example, molecules **1** and **3**, which show very similar PIC responses, differ in electronic structure and light absorption (**1** is a chromophore). All five molecules consist of carbon, nitrogen, and oxygen (and two sulfur atoms), therefore their molecular weight generally correlates with molecular size, and (for a similar surface coverage) with the monolayer thickness. The effective refractive index of the contacting medium, which in this case consists of the monolayer and surrounding air, is therefore expected to rise as a function of the monolayer thickness (see, for example, ref. [33]); this provides an explanation for the result in Figure 10.

  0947-6539/02/0817-3855 $ 20.00+.50/0

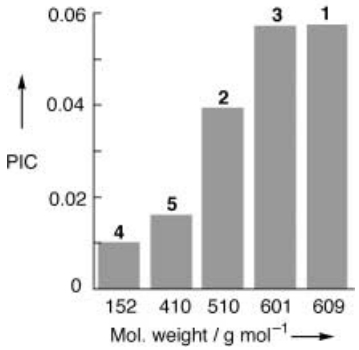

Figure 10. The Au PIC obtained for SAMs of molecules **1**–**5** adsorbed from 2 mM solutions in $CHCl_3$ (**1**–**3**, **5**) or in $CHCl_3$/EtOH (1:1) (**4**) for 40 min. The PIC values are an average of four samples. The Au substrates were 2.5 nm (nominal thickness) on mica, unannealed.

Conclusion

Ultrathin (1–10 nm thick) gold island films evaporated on transparent substrates can be used for quantitative monitoring of adsorption on the gold surface, by using UV/Vis spectroscopy in the transmission mode. Changes in the intensity (PIC) and wavelength of the Au surface plasmon band are observed upon binding of various species to the Au surface or to a receptor layer on the Au surface. The presence of a chromophore in the binding molecule does not seem to affect the amplitude of the PIC. As previously shown,[18] the PIC correlates approximately linearly with the surface coverage, suggesting possible use of T-SPR spectroscopy in chemical or biological sensing. The T-SPR method is highly versatile, allowing application in the liquid or gas phase, as well as semiquantitative in situ measurements at a single wavelength. T-SPR is relatively simple and inexpensive, with a sensitivity comparable to that of SPR. The transmission configuration is highly suitable for simultaneous measurements of multireceptor arrays.

Experimental Section

Chemicals: Molecules **1**, **3**, **5** were a gift from R. Lazar and Prof. A. Shanzer (Weizmann Institute). The synthesis of molecule **2** (Figure 3) was previously described.[31] Cobalt(II) tetraphenylporphyrin (CoTPP, Aldrich), 1-decanethiol ($C_{10}SH$, Aldrich), and ±-*trans*-1,2-dithiane-4,5-diol (Aldrich) (**4**) were used without further purification. Chloroform (Biolab, AR), ethanol (Merck, AR), 2,2,2-trifluoroethanol (TFE) (Fluka, AR), benzene (Biolab, AR), and pyridine (Biolab, AR) were used as received. Gas used was purified nitrogen (in house system).

Gold film preparation: Ultrathin gold films (1.3–10 nm nominal thickness) were prepared by mounting freshly cleaved mica or extensively rinsed (with ethanol) quartz slides in a cryo-HV evaporator (Key High Vacuum) equipped with a Maxtek TM-100 thickness monitor. Homogeneous deposition was obtained by moderate rotation of the substrate plate. Gold (99.99%) was evaporated from a tungsten boat at 4–5 $\times 10^{-6}$ Torr, at a deposition rate of 0.005–0.01 nm s^{-1}. Post-deposition annealing of evaporated Au-covered slides was carried out in air, either at 250 °C for 4 h or at 350 °C for 12 h. The heating rate was 5 °C min^{-1}, and the slides were left to cool in air to room temperature.

Preparation of organic layers: Monolayers of **1**, **2**, **3**, and **5** were adsorbed on the Au substrates from 2 mM solutions of the corresponding molecules in $CHCl_3$. Monolayers of **4** were adsorbed from a 2 mM $CHCl_3$/EtOH (1:1) solution of the molecule. Monolayers of $C_{10}SH$ were adsorbed from a 2 mM solution of the molecule in TFE. All the monolayers were rinsed successively with the solvent used for the adsorption and with absolute ethanol, then dried under a stream of purified nitrogen. Gas phase adsorption was initiated by placing a drop of the neat adsorbate in the spectroscopic cuvette containing the measured Au substrate.

UV/Vis spectroscopy: Measurements were carried out with a Jasco V-570 UV/Vis/NIR spectrophotometer. All ex situ measurements were performed in air using a specially designed cell. In situ measurements were carried out in a closed cuvette filled with the proper solution (measurements in liquid phase) or saturated with vapors of the chosen substance (measurements in gas phase). The scan speed was 100 nm min^{-1}. The bandwidth of the light source in the UV/Vis region was 5 nm. A baseline correction procedure was executed prior to each measurement session. All the spectra shown (unless otherwise stated) are difference spectra; the same slide was always used for obtaining the spectrum and for background subtraction. For the island films of $\leq$10 nm used in the present study, the intensity of scattered light is negligible compared to the absorption.[34] Therefore, the experimentally measured values of light extinction are presented as absorption. In the case of self-assembled monolayers (SAMs) of **1**–**5** the background was the bare gold. In the case of CoTPP bound to a SAM of **2**, the background was the gold with a SAM of **2**.

Atomic force microscopy (AFM): AFM images were recorded in air using a Topometrix 2010 Discoverer instrument operated in the non-contact mode. Commercial etched silicon probes, with a resonant frequency of about 428 kHz, were used.

Contact angle (CA) measurements: CAs were measured with a telescope-goniometer (Rame-Hart 100) at an estimated accuracy of ±2°. Advancing water CAs are reported.

Environmental scanning electron microscope (E-SEM) imaging: Images were obtained with a SEI-FEG E-SEM XL30 instrument.

Acknowledgements

Support from the Israel Science Foundation and the Minerva Foundation, Munich, is gratefully acknowledged. A.V. is partially supported by a Gileadi Fellowship of the Israel Ministry of Absorption. M.A.S. was supported by a Minerva Postdoctoral Fellowship. We thank R. Lazar and Prof. A. Shanzer for the synthesis of the molecules **1**, **3**, and **5**, and Dr. G. Ashkenasy and Prof. A. Shanzer for the synthesis of molecule **2**. Special thanks to Dr. E. Klein for the E-SEM imaging.

[1] S. Norman, T. Anderson, C. G. Granqvist, O. Hunderi, *Phys. Rev. B* **1978**, *18,* 674–695.
[2] O. Hunderi, *Surf. Sci.* **1980**, *96,* 1–31.
[3] T. Kuwana, N. Winograd in *Electroanalytical Chemistry, Vol. 7* (Ed.: A. J. Bard), Marcel Dekker, New York **1974**.
[4] W. R. Heineman, F. M. Hawkridge, H. Blount in *Electroanalytical Chemistry, Vol. 13* (Ed.: A. J. Bard), Marcel Dekker, New York **1984**.
[5] P. A. Di Milla, G. P. Lopez, J. P. Folkers, H. A. Biebuyck, R. Harter, G. M. Whitesides, *J. Cell. Biochem.* **1994**, 248–248.
[6] P. A. Di Milla, J. P. Folkers, H. A. Biebuyck, R. Harter, G. P. Lopez, G. M. Whitesides, *J. Am. Chem. Soc.* **1994**, *116,* 2225–2226.
[7] T. A. Postlethwaite, J. E. Hutchison, K. W. Hathcock, R. W. Murray, *Langmuir* **1995**, *11,* 4109–4116.
[8] K. Shimazu, M. Takechi, H. Fujii, M. Suzuki, H. Saiki, T. Yoshimura, K. Uosaki, *Thin Solid Films* **1996**, *273,* 250–253.
[9] J. E. Hutchison, T. A. Postlethwaite, C. H. Chen, K. W. Hathcock, R. S. Ingram, W. Ou, R. W. Linton, R. W. Murray, D. A. Tyvoll, L. L. Chng, J. P. Collman, *Langmuir* **1997**, *13,* 2143–2148.
[10] K. Uosaki, T. Kondo, X. Q. Zhang, M. Yanagida, *J. Am. Chem. Soc.* **1997**, *119,* 8367–8368.
[11] D. A. Offord, S. B. Sachs, M. S. Ennis, T. A. Eberspacher, J. H. Griffin, C. E. D. Chidsey, J. P. Collman, *J. Am. Chem. Soc.* **1998**, *120,* 4478–4487.
[12] N. Nishimura, M. Ooi, K. Shimazu, H. Fujii, K. Uosaki, *J. Electroanal. Chem.* **1999**, *473,* 75–84.

  0947-6539/02/0817-3856 $ 20.00+.50/0

[13] H. Imahori, H. Norieda, Y. Nishimura, I. Yamazaki, K. Higuchi, N. Kato, T. Motohiro, H. Yamada, K. Tamaki, M. Arimura, Y. Sakata, *J. Phys. Chem. B* **2000**, *104,* 1253 – 1260.
[14] Z. J. Zhang, R. S. Hu, Z. F. Liu, *Langmuir* **2000**, *16,* 1158 – 1162.
[15] G. Kalyuzhny, A. Vaskevich, S. Matlis, I. Rubinstein, *Rev. Anal. Chem.* **1999**, *18,* 237 – 242.
[16] G. Kalyuzhny, A. Vaskevich, G. Ashkenasy, A. Shanzer, I. Rubinstein, *J. Phys. Chem. B* **2000**, *104,* 8238 – 8244.
[17] P. Orfanides, T. F. Buckner, M. C. Buncick, F. Meriaudeau, T. L. Ferrell, *Am. J. Phys.* **2000**, *68,* 936 – 942.
[18] G. Kalyuzhny, M. A. Schneeweiss, A. Shanzer, A. Vaskevich, I. Rubinstein, *J. Am. Chem. Soc.* **2001**, *123,* 3177 – 3178.
[19] H. Raether, *Surface Plasmons on Smooth and Rough Surfaces and on Gratings*, Springer, Berlin **1988**.
[20] W. Knoll, *Annu. Rev. Phys. Chem.* **1998**, *49,* 569 – 638.
[21] D. K. Kambhampati, W. Knoll, *Curr. Opin. Colloid Interface Sci.* **1999**, *4,* 273 – 280.
[22] J. Homola, S. S. Yee, G. Gauglitz, *Sens. Actuators B* **1999**, *54,* 3 – 15.
[23] M. Gluodenis, C. Manley, C. A. Foss, *Anal. Chem.* **1999**, *71,* 4554 – 4558.
[24] M. Himmelhaus, H. Takei, *Sens. Actuators B* **2000**, *63,* 24 – 30.
[25] T. Okamoto, I. Yamaguchi, T. Kobayashi, *Opt. Lett.* **2000**, *25,* 372 – 374.
[26] J. C. Hulteen, D. A. Treichel, M. T. Smith, M. L. Duval, T. R. Jensen, R. P. Van Duyne, *J. Phys. Chem. B* **1999**, *103,* 3854 – 3863.
[27] M. D. Malinsky, K. L. Kelly, G. C. Schatz, R. P. Van Duyne, *J. Am. Chem. Soc.* **2001**, *123,* 1471 – 1482.
[28] F. Meriaudeau, T. R. Downey, A. Passian, A. Wig, T. L. Ferrell, *Appl. Optics* **1998**, *37,* 8030 – 8037.
[29] F. Meriaudeau, T. Downey, A. Wig, A. Passian, M. Buncick, T. L. Ferrell, *Sens. Actuators B* **1999**, *54,* 106 – 117.
[30] Throughout the text, the term ′annealed′ refers to films annealed at 250 °C for 4 h.
[31] G. Ashkenasy, G. Kalyuzhny, J. Libman, I. Rubinstein, A. Shanzer, *Angew. Chem.* **1999**, *111,* 1333 – 1336; *Angew. Chem. Int. Ed. Engl.* **1999**, *38,* 1257 – 1261.
[32] G. Ashkenasy, A. Ivanisevic, R. Cohen, C. E. Felder, D. Cahen, A. B. Ellis, A. Shanzer, *J. Am. Chem. Soc.* **2000**, *122,* 1116 – 1122.
[33] D. E. Aspnes, *Thin Solid Films* **1982**, *89,* 249 – 262.
[34] W. Caseri, *Macromol. Rapid Commun.* **2000**, *21,* 705 – 722.

Received: February 21, 2002 [F3891]

  0947-6539/02/0817-3857 $ 20.00+.50/0